Sequence-Specific Double-Strand Cleavage of DNA by Fe−Bleomycin. 2. Mechanism and Dynamics†

M. J. Absalon,‡ W. Wu,‡ J. W. Kozarich,*,§ and J. Stubbe*,‡

Departments of Chemistry and Biology, Massachusetts Institute of Technology, Cambridge, Massachusetts 02139, and Department of Chemistry and Biochemistry, University of Maryland, College Park, Maryland 20742

Received August 9, 1994; Revised Manuscript Received November 14, 1994®

ABSTRACT: The mechanism of iron−bleomycin-mediated ds-cleavage of DNA has been investigated at specific sites within specific sequences using hairpin oligonucleotides (Absalon et al., 1995) and our recently developed technique for determining sequence-specific isotope effects upon oxidative degradation of DNA (Kozarich et al., 1989; Worth et al., 1993). Isotope effects upon ds-cleavage have been observed when the C-4′ hydrogen of either nucleotide involved in the ds-break was substituted with deuterium. The values of the isotope effects determined for ss and ds events occurring at the same site were indistinguishable at four sites examined in detail. The results are consistent with a mechanism of ds-cleavage in which the pathways leading to ss- and ds-cleavage partition from a common intermediate subsequent to abstraction of the C-4′ hydrogen from the first nucleotide involved in the cleavage. Deuterium substitution at the primary cleavage site of a ds-break failed to result in an equivalent effect on the amount of cleavage at the secondary cleavage site, suggesting that ds-cleavage may be initiated from either of the nucleotides involved in the ds-cleavage event. A kinetic preference for cleavage initiated at the 1° site, however, is probable. The requirement in the ds-cleavage process for O_2, in addition to that needed to form "activated BLM", has been clearly demonstrated by the absence of ds-cleavage products in reactions performed under anaerobic conditions in which ss-cleavage still occurs. These results support, in part, the basic model for ds-cleavage proposed by Steighner and Povirk [(1990) *Proc. Natl. Acad. Sci. U.S.A. 87,* 8350−8354], in which a single molecule of BLM effects ds-cleavage and requires reactivation to effect cleavage at the second strand. The essential factor establishing the ratio of ss- to ds-cleavage at a specific site may be related to the efficiency by which Fe-BLM can be reactivated and/or repositioned at a second site for cleavage.

Studies evaluating the extent of single-strand (ss)[1] and double-strand (ds) DNA cleavage mediated by bleomycin (BLM) necessitate the consideration of a mechanism for ds-cleavage in which a single molecule of BLM is responsible for both strand breaks (Absalon et al., 1995; Povirk et al., 1977). Incubation of BLM with Fe^{2+} and O_2 yields a mixture of ferric−BLM and "activated BLM", a species recently shown by electrospray mass spectrometry to be BLM−ferric−peroxide which is kinetically competent to cause both ss- and ds-cleavage (Burger et al., 1981, 1986; Sam et al, 1994). However, in contrast to the enediyne family of antibiotics which are proposed to cause ds-breaks via a diradical form of the drug (Dedon and Goldberg, 1992), "activated BLM" possesses only a single reactive moiety. Furthermore, a recent detailed analysis of the sequence specificity of BLM-induced ds-breaks (Povirk et al., 1989; Steighner and Povirk, 1990) has revealed that the individual nucleotides involved in cleavage are predominantly 5′-staggered by one nucleotide or, alternatively, blunt-ended to each other—a pattern which is unusual for DNA cleavage agents proposed to mediate chemistry from the minor groove (Dervan, 1986). The distance between the two cleavage sites (15−18 Å) and the apparent lack of bifunctionality of "activated BLM" thus present an apparent impasse that has prompted us to apply our technology for the assessment of sequence-specific isotope effects to the hairpin oligonucleotides described in the preceding paper (Absalon et al., 1995), and to quantitatively investigate a number of proposals regarding the ds-cleavage process mediated by Fe-BLM.

Recent experiments of Steighner and Povirk (1990), using native polyacrylamide gel electrophoresis (PAGE) have allowed identification of ~30 BLM-induced ds-cleavage sites. A reanalysis of five of these sites using denaturation PAGE has allowed Povirk and co-workers (1989) to propose sequence-dependent selection rules and several mechanisms for the ds-cleavage process. One site of the ds-break has been designated the primary (1°) site and is a prominent ss-cleavage site as previously defined by numerous investigators (D'Andrea and Haseltine, 1978; Sugiura and Suzuki, 1982; Kuwahara and Sugiura, 1988; Fox, 1990). The second site was termed the secondary (2°) site and bears no resemblance to the reported selectivity for FeBLM ss-cleavage. Cleavage at the 2° site was only observed in the context of ds-cleavage; therefore, it was suggested that degradation at the 1° site was a requirement for cleavage to occur at the 2° site. On the basis of the electrophoretic migration of [5′-^{32}P]-labeled

† This work was supported by NIH Grant GM 34454 to J.W.K. and J.S.

* Authors to whom correspondence should be addressed.

‡ Massachusetts Institute of Technology.

§ University of Maryland.

® Abstract published in *Advance ACS Abstracts,* January 1, 1995.

[1] Abbreviations: ss, single-strand; ds, double-strand; BLM, bleomycin; PAGE, polyacrylamide gel electrophoresis; 1°, primary; 2°, secondary; PCR, polymerase chain reaction; TBE buffer, Tris-HCl (pH 8), 89 mM boric acid, and 2 mM EDTA; HEPES, *N*-(2-hydroxyethyl)-piperazine-*N*′-2-ethanesulfonic acid.

0006-2960/95/0434-2076$09.00/0

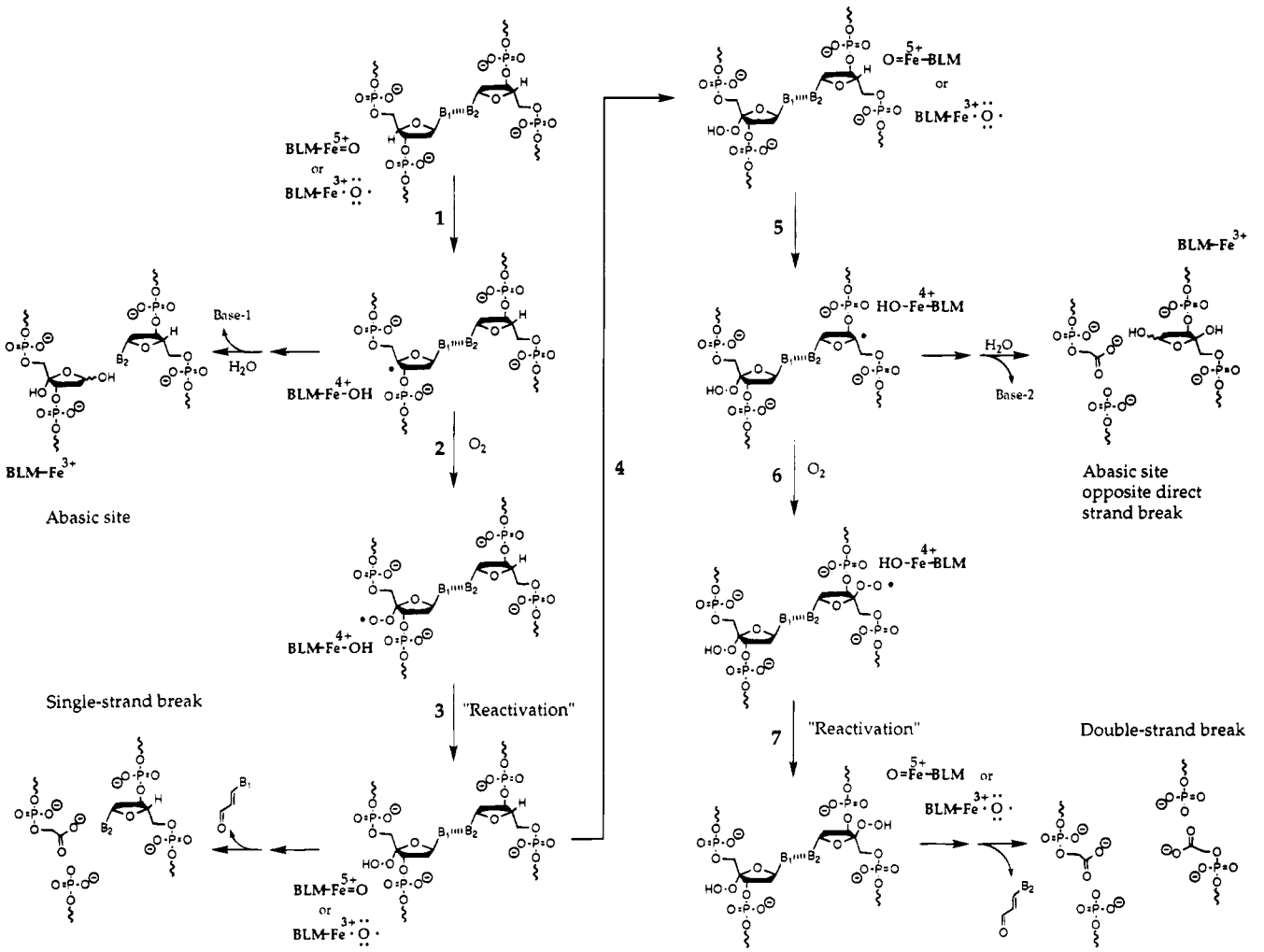

FIGURE 1: Proposed mechanism for Fe-BLM-mediated ds-cleavage.

products of ds-cleavage on denaturing gels, 1° site cleavages appeared to only yield fragments with 3′-phosphoglycolate modified ends, while cleavage at the 2° sites resulted in fragments with either 3′-phosphoglycolate or 3′-phosphate ends, the latter being produced subsequent to "alkaline" treatment. The putative 3′-phosphoglycolate-modified ends suggested that the chemistry of ds-cleavage involves C-4′ hydrogen abstraction at both sites in a process analogous to that previously determined for ss-cleavage (Wu et al., 1985; Kozarich et al., 1989; Stubbe and Kozarich, 1987). In addition, the observation of the exclusive formation of 3′-phosphoglycolate ends at the 1° site implied a requirement for oxygen above that needed to form "activated BLM", in producing ds-breaks. These studies resulted in a proposal of several models for BLM-mediated ds-cleavage. The first model requires reactivation of Fe(III)-BLM by a putative C-4′ hydroperoxide intermediate. However, regardless of whether the reactivation involves homolytic or heterolytic oxygen−oxygen bond scission, neither process is consistent with the formation of the observed 3′-phosphoglycolate moieties at the 1° site.

The following is our interpretation of the second model suggested by Steighner and Povirk (1990), which has functioned as our working hypothesis for the studies reported in this paper. An activated Fe-BLM species abstracts the C-4′ hydrogen from a good ss-cleavage site (1° site), to generate a C-4′ radical (Figure 1). For a ds-break to be observed, this radical must be trapped with O_2 to form a C-4′ peroxyl radial. This intermediate is then reduced by the BLM product of the first hydrogen abstraction (BLM-Fe^{IV}-OH) to generate the C-4′ hydroperoxide and a BLM−iron−oxene. The hydroperoxide leads to strand scission and eventually to formation of base−propenal and a fragment with a 3′-phosphoglycolate-modified end. The resulting iron−oxene can then be used to abstract a second hydrogen atom from the C-4′ position of another nucleotide on the opposite strand (2° site). The resulting C-4′ radical at this second site could then partition, depending upon the O_2 concentration, to eventually give a 3′-phosphoglycolate end or an abasic site which leads to a 3′-phosphate end subsequent to base treatment.

The model in Figure 1 makes a number of predictions which can be tested experimentally. First, the model relies upon a single molecule of Fe-BLM to effect both cleavage events. Studies presented in the preceding paper attempted to address this issue, and while the results supported this hypothesis, a description of the dramatic rearrangement required of this single molecule of Fe-BLM has yet to be offered. Second, the model predicts that C-4′ hydrogen abstraction occurs at both the 1° and 2° cleavage sites. While the electrophoretic migration of the ds-cleavage products on denaturing gels has been reasonably interpreted as being representative of C-4′ chemistry (Steighner & Povirk, 1990), the correlative nature of these investigations requires further

support for C-4′ carbon−hydrogen bond cleavage. We have therefore applied our recently developed technique for observing sequence-specific isotope effects upon DNA cleavage (Kozarich et al., 1989; Worth et al., 1993), to confirm that cleavage at both sites of a double-strand break involves C-4′ hydrogen abstraction. Third, the model predicts that there is an obligate order to the ds-cleavage event which explains the occurrence of 2° site cleavage. Most studies on ss-cleavage have focused on the "major" hit sites and have ignored the cleavage occurring at minor hit sites. Since the frequency of cleavage at many of these minor hit sites is similar to that for ds-cleavage (10−20% of the major cleavage events), it has been tempting to generally attribute their occurrence to ds-cleavage. Previous studies with DNA homopolymer duplexes, however, have indicated that cleavage by Fe-BLM can occur on both strands (Absalon et al., 1992; Krishnamoorthy et al., 1988), neither of which possesses good 1° cleavage sites. Therefore, to determine the involvement of 2° site degradation in ss- and ds-cleavage, we have reinvestigated the order of the individual cleavage events leading to a ds-break by evaluating the effect of deuterium substitution at 1° sites upon the cleavage observed at the corresponding 2° sites. Measurement of these isotope effects suggests that one mode of binding may be responsible for both ss- and ds-cleavage events. Finally, the model of Povirk and co-workers dictates an absolute requirement for O_2 in a ds-cleavage event above that required for generation of activated BLM. Therefore, the oxygen requirement has been directly evaluated by monitoring ds-cleavage under anaerobic conditions. Our results support the mechanism shown in Figure 1 and offer a possible explanation for the differences observed in the efficiency of ds-cleavage at individual sites.

EXPERIMENTAL PROCEDURES

Materials. Amplitaq polymerase was purchased from Perkin-Elmer-Cetus. *Eco*RI and *Mlu*I were purchased from New England Biolabs. [4′-^{2}H]TTP and [4′-^{2}H]dCTP were prepared as previously described (Ajmera et al., 1986; Kozarich et al., 1989). [4′-^{2}H]Adenosine was prepared using *S*-adenosylhomocysteine hydrolase and converted to the triphosphate as previously described (Wu et al., 1985). All specifically deuteriated nucleotides were greater than 94% isotopically enriched as determined by ^{1}H-NMR integration. [5′-^{32}P]- and [i-^{32}P]-labeled hairpins (GT-1, GT-2, GA-1, and GC-1) were prepared as described in the preceding paper (Absalon et al., 1995).

Polymerase Chain Reaction (PCR) To Generate [^{1}H]- and [^{2}H]DNA. The 1.2-kb DNA fragment of pJS187 containing the restriction sites for *Mlu*I, *Eco*RI, and *Bgl*II was amplified by PCR technology using primers that flank the *Mlu*I/*Bgl*II restriction sites. Reactions were performed in 100 μL and contained 100 μM of each dNTP, 10 mM Tris-HCl (pH 8.3 at 25°C), 50 mM KCl, 1.5 mM $MgCl_2$, 0.01% w/v Sigma 6-2500 gelatin, 1 ng of pJS187 previously linearized using *Xba*I, and 2.5 units of Amplitaq polymerase. The primers, 5′-CGA-TCG-GTG-CGG-GCC-TCT-TCG and 5′-GTT-GCC-TTC-CGC-CGC-CAT-GC, were each present in 100 pmol quantities. For the preparation of specifically deuteriated DNA, [4′-^{2}H]dATP or [4′-^{2}H]TTP was substituted for the corresponding [^{1}H]dNTP. Reactions were overlaid with 100 μL of paraffin oil and heat-cycled 40 times in an Ericomp Single-Block device using the following program: 1 min at 94 °C, 2 min at 50 °C, and 2 min at 72 °C with the time period of incubation at 72 °C increased by 30 s after every set of 10 cycles until a maximum period of 3 min at 72 °C was reached. Reactions were completed with an additional cycle including 1 min at 94 °C, 5 min at 45 °C, and 10 min at 72 °C. The 1.2-kb PCR product was separated from the reaction mixture by electrophoresis through 1% agarose containing 1 μg/mL ethidium bromide using 89 mM Tris-HCl (pH 8), 89 mM boric acid, and 2 mM EDTA (TBE buffer) and excised from the gel by standard electroelution techniques (Sambrook et al., 1989). Ethidium bromide was separated from the purified DNA by 8 extractions with 100 μL of H_2O-saturated 1-butanol, and the sample was extracted once with phenol before concentration by ethanol precipitation. Samples were dissolved in 20 μL of 5 mM HEPES (pH 7.5) and 5 mM NaCl, and their concentration was determined by the A_{260} nm (1 A_{260} unit corresponds to 50 μg/mL ds-DNA). One PCR yielded 5−9 μg of the 1.2-kb fragment.

^{32}P-Labeling of DNA Fragments Prepared by PCR. 5′- and 3′-^{32}P labeling was performed at the *Eco*RI restriction site on ~5 μg of the 1.2-kb PCR product using standard techniques (Sambrook et al., 1989). A 740-bp ^{32}P-labeled fragment was produced by restriction digestion using ~50 units of *Mlu*I in 50 μL of the manufacturer-supplied buffer and purified using a 10% PAGE under nondenaturing conditions. Excision of the [^{32}P]DNA from the gel was performed as described above to yield (0.5−1.2) × 10^6 Cerenkov cpm of ^{32}P-labeled materials.

Fe-BLM Degradation of PCR Prepared DNA. Degradation of [^{1}H] and [^{2}H] 740-bp fragments by BLM was performed in a total volume of 25 μL containing 50 000−250 000 Cerenkov cpm of [^{32}P]-labeled DNA (specific activity (0.2−1) × 10^6 cpm μg^{-1}), 50 mM HEPES (pH 7.5), 50 mM NaCl, 32 μM $(Fe^{2+})(NH_4)_2(SO_4)_2$, 0.2 μg/μL salmon testes DNA, and 1.75 μM BLM. Reactions were initiated by the addition of the iron and allowed to incubate at room temperature for 10 min. Control reactions lacked BLM. Sucrose gel-loading buffer (5 μL) was added to each reaction which was analyzed by 20% native PAGE (gel dimensions: 43 cm × 38 cm × 0.4 mm) employing 400−700 V constant potential for ~36 h, in a 4 °C room (Sambrook et al., 1989). Gels were visualized using a Molecular Dynamics PhosphorImager.

Preparation of [^{2}H]Hairpin Oligonucleotides. [^{2}H]-[5′-^{32}P]- and -[i-^{32}P]oligonucleotides, and their [^{1}H] counterparts, were prepared in parallel by procedures analogous to those reported in the preceding paper (Absalon et al., 1995). For GT-1 and GT-2, [4′-^{2}H]TTP was used in place of the [^{1}H]-TTP, while [4′-^{2}H]dATP was used for the preparation of GA-1 and [4′-^{2}H]dCTP for GC-1.

Degradation of [^{1}H]- and [^{2}H]Hairpin Oligonucleotides by Fe-BLM: Determination of Site-Specific Isotope Effects. The Fe-BLM degradation reactions were performed identically and in parallel for a given pair of [^{32}P]-[^{1}H]- and -[^{2}H]-hairpin oligonucleotides. A typical reaction contained, in a final volume of 80 μL, [^{32}P]oligonucleotide (~120 000 Cerenkov cpm), 16 μg of salmon testes DNA, 50 mM HEPES (pH 7.5), and 50 mM NaCl. The reaction solution was heated to 95 °C for 2 min and cooled to room temperature over a 1 h period before being further cooled to 4 °C. "Activated BLM" was formed *ex situ* as previously described (Absalon et al., 1995), and an appropriate aliquot

was added to give final concentrations between 14 and 80 μM in Fe-BLM. Control reactions omitted Fe-BLM. The reactions were incubated for 10 min at 4 °C, and the DNA was isolated by ethanol precipitation with 80 μL of 0.6 M NaOAc and 900 μL of ethanol. The precipitated samples were dissolved in 20 μL of formamide gel-loading buffer, and the amount of Cerenkov radiation was determined for each sample. Reaction samples were loaded onto a 20% polyacrylamide sequencing gel, taking care that all lanes received approximately equal amounts of [^{32}P]-labeled material. Electrophoresis was carried out with 80 W of constant power for 3−5 h. [^{32}P] products were visualized and quantified using a Molecular Dynamics PhosphorImager equipped with *Image Quant* software (version 3).

Oxygen-Dependent Ds-Cleavage by Fe-BLM. [i-^{32}P]- or [5′-^{32}P]GT-1 or -GT-2 (700 000 Cerenkov cpm), 112 μg of salmon testes DNA, 57 mM HEPES (pH 7.5), and 57 mM NaCl in a final volume of 490 μL was annealed as described above. The solution was divided into six 70 μL aliquots and placed into borosilicate glass culture tubes (6 mm × 50 mm) and an appropriate volume of H_2O added such that upon the addition of Fe-BLM the final volume would be 80 μL. Samples to be deoxygenated were stoppered with a septum and attached to a vacuum manifold via an 18-gauge needle. Each of the solutions was frozen in a dry-ice/acetone bath and the system evacuated. Each solution was then thawed *in vacuo* and repressurized with argon. This process was repeated 4−5 times. These samples and three controls not subjected to deoxygenation were chilled to 4 °C for 15 min. "Activated BLM" was prepared *ex situ* (Absalon et al., 1995), and a 5 or 10 μL aliquot was added to each reaction solution under an argon atmosphere. Reactions were incubated at 4 °C for 10 min and then stopped by the addition of 80 μL of 0.6 M NaOAc. The solutions were then divided into two 80 μL aliquots to which 800 μL of ethanol was added, and the DNA was isolated by standard procedures. One sample was dissolved in 100 μL of 1 M piperidine and incubated at 95 °C for 15 min. Alternatively, the sample was dissolved in 100 μL of 10 mM putrescine (pH 8) and incubated at 37 °C for 1 h. The DNA was isolated from each sample by ethanol precipitation and then dissolved in 20 μL of formamide gel loading buffer. The [^{32}P] products were separated by electrophoresis under denaturing conditions using a 20% polyacrylamide gel.

RESULTS

Isotope Effects on Fe-BLM-Mediated Ds-Cleavage of the EcoRI/MluI Fragment of pJS187. The model shown in Figure 1 proposes that chemistry at both the 1° and 2° sites of a ds-break occurs with C-4′ hydrogen abstraction. Our past studies on the mechanism of ss-cleavage mediated by Fe-BLM have revealed that this process is accompanied by an isotope effect when deuterium is substituted for the C-4′ hydrogen of a targeted nucleotide, resulting in a reduction in the amount of a cleavage product observed upon analysis via sequencing gels (Kozarich et al., 1989; Worth et al., 1993). To determine if site-specific ds-cleavage by Fe-BLM is also affected by C-4′ deuterium substitution at either the 1° of 2° cleavage sites, we prepared the *Eco*RI/*Mlu*I fragment of pJS187 in which all of the dA or T nucleotides were substituted with [^{2}H] at the C-4′ position. These specifically [^{2}H]-labeled restriction fragments were [^{32}P]-labeled at the 3′- or 5′-ends and treated with Fe-BLM, and the ds-cleavage products were separated by nondenaturing PAGE. Several of the ds-cleavage fragments were isolated from the gel and

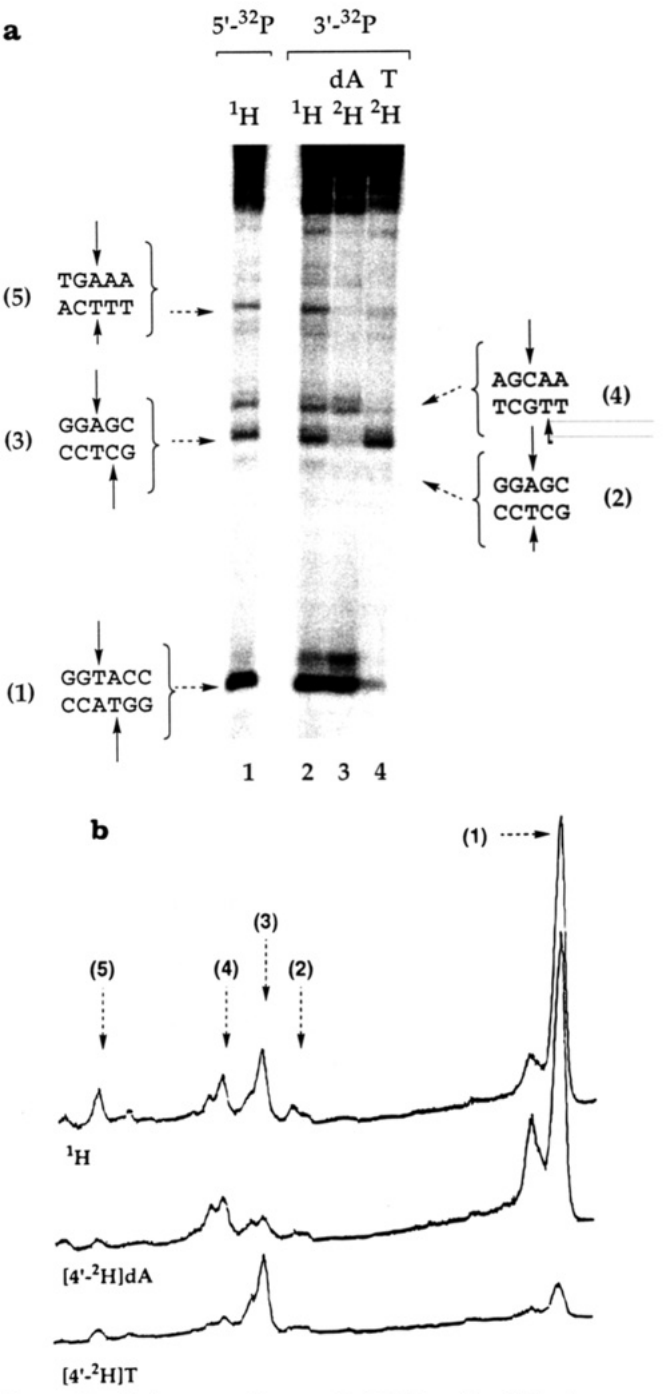

FIGURE 2: (a) Isotope effects on Fe-BLM-mediated ds-cleavage of the *Eco*RI/*Mlu*I fragment of pJS187. The [^{1}H] and [^{2}H] *Eco*RI/*Mlu*I fragments of pJS187 were prepared using PCR, and 3′-^{32}P-labeled at the *Eco*RI site. [^{1}H]DNA was also 5′-^{32}P-labeled at the *Eco*RI site. The [^{1}H] and [^{2}H] fragments were treated with 1.75 μM BLM and 32 μM ferrous ammonium sulfate at room temperature for 10 min before analysis using a 20% polyacrylamide gel run under nondenaturing conditions. Lane 1 contains [5′-^{32}P]-[^{1}H] DNA. Lane 2 contains [3′-^{32}P]-[^{1}H]DNA. Lane 3 contains [3′-^{32}P]-DNA prepared using [4′-^{2}H]dATP. Lane 4 contains [3′-^{32}P]DNA prepared using [4′-^{2}H]TTP. (b) Histograms of Fe-BLM-mediated degradation reactions of [^{1}H] and [^{2}H] *Eco*RI/*Mlu*I fragment of pJS187. PhosphorImager-generated histograms of the [^{1}H]- and [4′-^{2}H]dA DNA fragments (numbered in parentheses) shown in panel a were normalized using the area corresponding to ds-cleavage at fragment **1**. [^{1}H]- and [4′-^{2}H]T reaction profiles were normalized using the area corresponding to ds-cleavage at fragment **3**.

Table 1: Approximate Values for the Isotope Effects Observed upon Ds-Cleavage in the *Eco*RI/*Mlu*I Fragment of pJS187[a]

ds-cleavage site	fragment no.	k_H/k_D for [4′-^{2}H]dA	k_H/k_D for [4′-^{2}H]T
5′-GTAC	**1**	(1)[b]	6-8
3′-CATG			
5′-GGAGC	**2**	3-4	4
3′-CCTCG			
5′-GGAGC	**3**	3-4	(1)[c]
3′-CCTCG			
5′-AGCAA	**4**	1-1.5	3
3′-TCGTT			
5′-TGAAA	**5**	3-4	2-3
3′-ACTTT			

[a] Experiments used [3′-^{32}P]DNA. [b] Fragment **1** was used for normalization in determining the [4′-^{2}H]dA isotope effects. [c] Fragment **3** was used for normalization in determining the [4′-^{2}H]T isotope effects.

reanalyzed on a denaturing gel, allowing their sequence identity to be inferred from their relative migration compared to Maxam–Gilbert standards. The results of one degradation experiment are shown in Figure 2a, and the corresponding PhosphorImager-generated histograms for the individual lanes are shown in Figure 2b. Isotope effects upon ds-cleavage are observed at all of the sites in which a deuterium is located at the C-4′ position of either the 1° or 2° sites of cleavage. Fragments **2** and **5**, both of which are composed of dA 1° sites and T 2° sites, exhibit isotope effects. Similarly, an isotope effect is also observed on ds-cleavage at 5′-AGCAA/ 5′-TTGCT (fragment **4**) when the 2° site (T) is deuteriated.

Immediately apparent in Figure 2 is the existence of a very large isotope effect (6–8, Table 1) upon ds-cleavage at the 5′-GTAC/5′-GTAC site (fragment **1**) when the C-4′ position of T is deuteriated. Since both thymidines contain a [4′-^{2}H], the isotope effect is likely to be the product of two isotope effects, one for each cleavage event involved in producing the ds-break.

The histogram shown in Figure 2b also reveals the limitations in the use of nondenaturing PAGE to evaluate sequence-specific isotope effects upon ds-cleavage. Due to the low abundance of ds-cleavage products relative to the background signal and due to poor resolution of the products, it is difficult to assign reliable values to the isotope effects observed. Only for site **1** do these concerns not pose a significant problem. Only approximate values for the isotope effects upon ds-cleavage can be reported for the other sites. The values, listed in Table 1, reveal that, despite these limitations, C-4′ chemistry occurs at both the 1° and 2° sites involved in a ds-cleavage event.

Isotope Effects upon Ss- and Ds-Cleavage of Hairpin Oligonucleotides: GT-1, GT-2, GA-1, and GC-1. The difficulties encountered with quantitation using the nondenaturing PAGE method and our inability to measure isotope effects simultaneously on ss- and ds-cleavage events were the driving force for the development of a new method to examine ds-cleavage using hairpin oligonucleotides. Hairpin oligonucleotides GT-1, GT-2, GC-1, and GA-1 were prepared

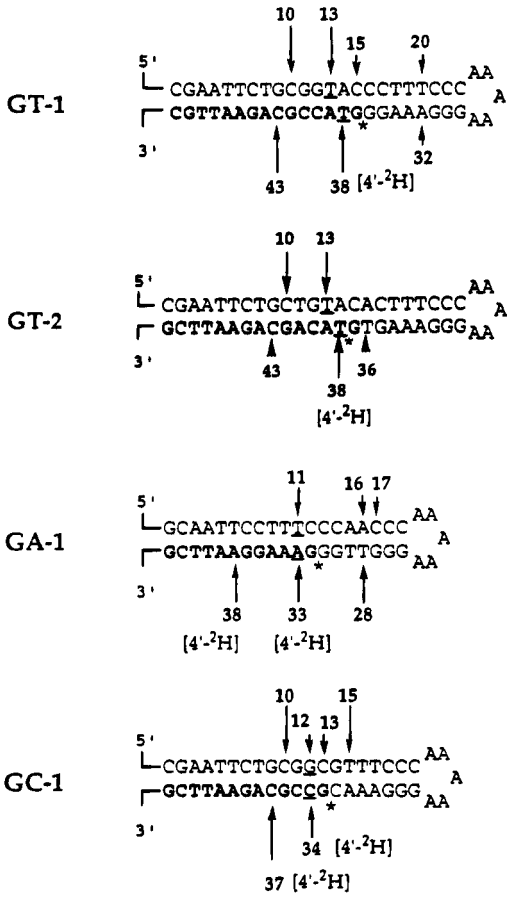

FIGURE 3: [^{1}H]- and [^{2}H]hairpin oligonucleotides. The phosphodiester bonds containing the "internal" ^{32}P-label are indicated with a (*), and the portion synthesized by the primer-extension is shown in bold type. The cleavage sites which were substituted with deuteriated nucleotides are labeled with "[4′-^{2}H]". The observed sites of cleavage by Fe-BLM are indicated with arrows, and the nucleotides involved in ds-cleavage are shown underlined.

as previously described (Absalon et al., 1995), with [4′-^{2}H] incorporated into the nucleotides as shown in Figure 3. The corresponding [^{1}H]oligonucleotides were prepared in parallel. The results of an experiment in which [i-^{32}P]GT-1 (^{1}H and ^{2}H) was incubated with "activated BLM" generated *ex situ* is shown in Figure 4a. A PhosphorImager-generated histogram for this gel is shown in Figure 4b, and the computed isotope effects for specific cleavage events are summarized in Table 2. The isotope effects upon ss-cleavage were also determined using [5′-^{32}P]GT-1, and the results are also included in Table 2. Using [i-^{32}P]GT-1, an isotope effect of 2.4 was determined for ss-cleavage at T_{38}, experimentally indistinguishable from the effect observed at the fragment resulting from ds-cleavage ($T_{13} + T_{38}$, $k_H/k_D = 2.3$). The cleavage at T_{38} observed when using [5′-^{32}P]GT-1 reflects only ss-cleavage at that site and should therefore yield an isotope effect identical to that observed for the corresponding ss-cleavage using [i-^{32}P]GT-1. However, the values obtained for cleavage at T_{38} with [5′-^{32}P]GT-1 are consistently higher (3.0 vs 2.4) and are believed to reflect a systematic difference in the methods of quantitation. With [i-^{32}P]GT-1, ss-cleavage occurring at C_{10} and C_{43} was used to normalize the [^{1}H]- and [^{2}H]oligonucleotide cleavage products so that a direct comparison between the two could be made. This fragment is large, 34 nucleotides, and consequently migrates at the top of the gel (Figure 4a,b) where interference is apparent

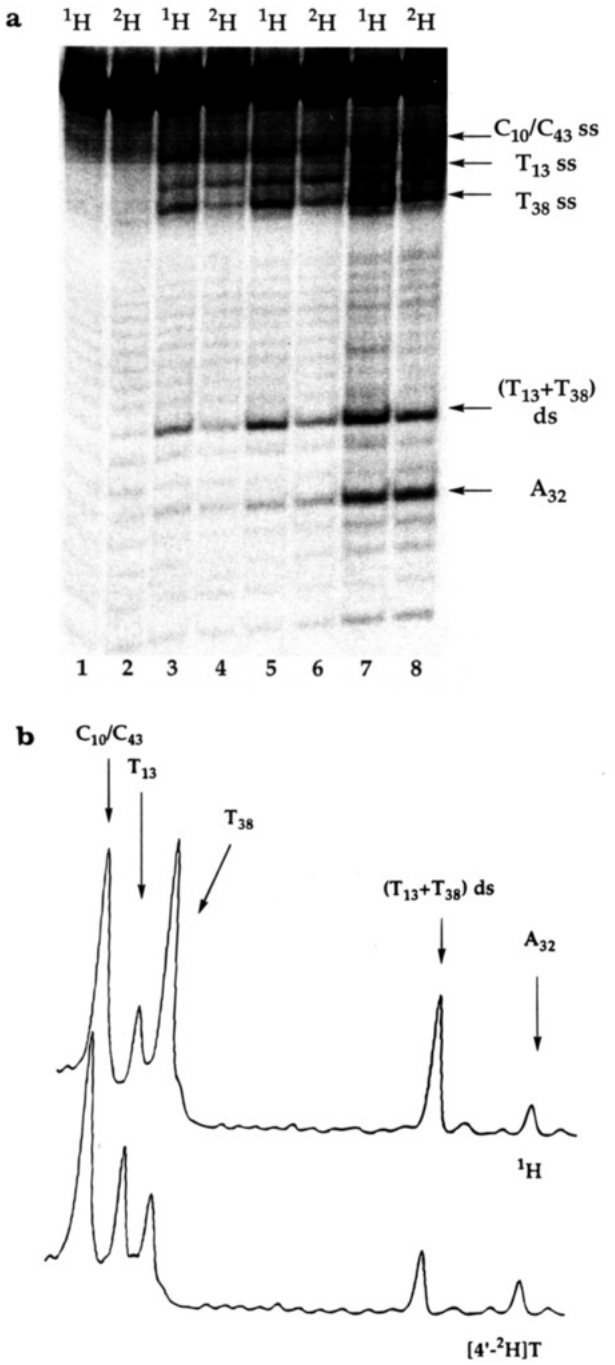

FIGURE 4: (a) Sequence-specific isotope effects on Fe-BLM degradation of [i-^{32}P]GT-1. [^{1}H]GT-1 and [^{2}H]GT-1 containing an internal ^{32}P-phosphodiester bond were treated with Fe-BLM and the products separated using a 20% polyacrylamide sequencing gel. Lanes labeled "^{1}H" and "^{2}H" contain [^{1}H]GT-1 and [^{2}H]GT-1, respectively. The concentration of Fe-BLM used in each reaction is as follows: lanes 1 and 2, no Fe-BLM; lanes 3 and 4, 7 μM Fe-BLM; lanes 5 and 6, 14 μM Fe-BLM; lanes 7 and 8, 28 μM Fe-BLM. The assignment of each fragment is denoted at right. (b) Histograms showing sequence-specific isotope effects on Fe-BLM degradation of [i-^{32}P]GT-1. PhosphorImager-generated histograms compare the fragmentation patterns for the reactions in lanes 5 and 6 shown in panel 4a. The two histograms were normalized upon the peak corresponding to ss-cleavage at C_{10} and C_{43}. (T_{38} is [4′-^{2}H], while T_{13} is not; see Experimental Procedures.)

from both uncut oligomers as well as other large fragments. In contrast, normalization for a comparison of the [^{1}H]- and [^{2}H]-[5′-^{32}P]-GT-1 is carried out using C_{10} (data not shown). This fragment is in a very clean region of the gel which facilitates accurate quantitation.

Table 2: Sequence-Specific Isotope Effects on Fe-BLM Cleavage of GT-1 Deuteriated at the C-4′ Position of T_{38}

^{32}P-label	cleavage site	% product distribution [^{1}H][a]	% product distribution [^{2}H][b]	k_H/k_D (av)[c]
internal	$C_{43} + C_{10}$ ss[d]	2.15	2.14	1.0
internal	T_{13} ss	1.27	1.26	0.9 ± 0.1
internal	T_{38} ss	2.18	0.94	2.4 ± 0.2
internal	($T_{13} + T_{38}$) ds	0.93	0.423	2.3 ± 0.3
internal	A_{32}	0.25	0.25	1.0 ± 0.3
5′	C_{43}	0.31	0.45	0.8 ± 0.2
5′	T_{38}	1.6	0.635	3.0 ± 0.2
5′	A_{32}	0.11	0.14	1.0 ± 0.1
5′	T_{13}	1.35	1.33	1.2 ± 0.1
5′	C_{10}[e]	1.02	1.13	1.0

[a] The product distribution shown is for one set of reactions employing 14 μM Fe-BLM. The total degradation of [^{1}H]-[i-^{32}P]GT-1 was 6.9%. The total degradation of [^{1}H]-[5′-^{32}P]GT-1 was 5.1%. [b] The product distribution shown is for one set of reactions employing 14 μM Fe-BLM. The total degradation of [^{2}H]-[i-^{32}P]GT-1 was 5.1%. The total degradation of [^{2}H]-[5′-^{32}P]GT-1 was 4.1%. [c] The average of 5 experiments employing 7−28 μM Fe-BLM. [d] The extents of cleavage observed with [i-^{32}P]GT-1 were normalized on the extent observed at this site. [e] The extents of cleavage observed with [5′-^{32}P]GT-1 were normalized on the extent observed at this site.

Table 3: Sequence-Specific Isotope Effects on Fe-BLM Cleavage of GT-2 Deuteriated at the C-4′ Position of T_{38}

^{32}P-labed	cleavage site	% product distribution [^{1}H][a]	% product distribution [^{2}H][b]	k_H/k_D (av)[c]
internal	C_{43}/C_{10} ss[d]	6.6	11.8	1.0
internal	T_{13} ss	5.3	9.9	0.8 ± 0.1
internal	T_{38} ss	6.2	4.6	2.4 ± 0.1
internal	($T_{13} + T_{38}$) ds	2.1	1.1	2.3 ± 0.7
5′	C_{43}	5.0	5.4	0.9 ± 0.1
5′	T_{38}	10.0	4.7	2.6 ± 0.3
5′	T_{13}	8.3	9.5	1.0 ± 0.1
5′	C_{10}[e]	4.7	5.3	1.0

[a] The total degradation of [^{1}H]-[i-^{32}P]GT-2 was 26%. The total degradation of [^{1}H]-[5′-^{32}P]GT-2 was 34%. All experiments were perfomed using 10 μM Fe-BLM. [b] The total degradation of [^{2}H]-[i-^{32}P]GT-2 was 35%. The total degradation of [^{2}H]-[5′-^{32}P]GT-2 was 31%. [c] The average of three experiments. The error represents the standard deviation. [d] The extents of cleavage observed with [i-^{32}P]GT-2 were normalized on the extent observed at this site. [e] The extents of cleavage observed with [5′-^{32}P]GT-2 were normalized on the extent observed at this site.

The isotope effects upon ss- and ds-cleavage in GT-2 (Figure 3), which differs from GT-1 only at the two base pairs surrounding the 5′-GTAC/5′-GTAC site, were also examined, and the results are presented in Table 3. Similar to the results obtained with GT-1, the isotope effects for ss- and ds-cleavage involving T_{38} of [i-^{32}P]GT-2 are indistinguishable (2.4 vs 2.3). In addition, an increase in the extent of ss-cleavage observed at T_{13} when T_{38} is deuteriated leads to an apparent "inverse" isotope effect (0.8, Table 3; a similar effect is seen in GT-1 at T_{13}, Table 2). This result is most likely a reflection of the reduced amount of ds-cleavage that occurs from a pathway in which initial degradation at T_{13} is normally followed by the cleavage at T_{38}. The reduced amount of a second cleavage event at [4′-^{2}H]T_{38} results in an increase in the ss-cleavage product from degradation at T_{13}. The results with GT-1 and GT-2 support the studies with the nondenaturing gels indicating the importance of C-4′ chemistry to the ds-cleavage process. In addition, the

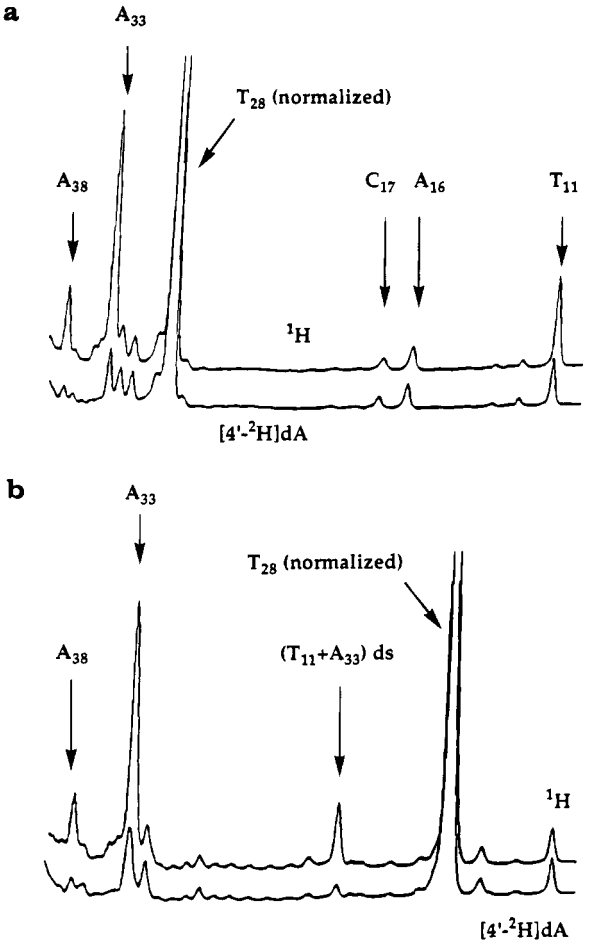

FIGURE 5: (a) Histograms showing sequence-specific isotope effects on Fe-BLM degradation of [5′-^{32}P]GA-1. [5′-^{32}P]-[^{1}H]- and -[^{2}H]-GA-1 were treated with 25 μM Fe-BLM and the products separated using a 20% polyacrylamide sequencing gel. The PhosphorImager-generated histograms were normalized upon the peak corresponding to cleavage at T_{28}. (A_{33} is [4′-^{2}H], while A_{16} is not; see Experimental Procedures.) (b) Histograms showing sequence-specific isotope effects on Fe-BLM degradation of [i-^{32}P]GA-1. [^{1}H]- and [^{2}H]GA-1 containing an internal ^{32}P phosphodiester bond were treated with 25 μM Fe-BLM and the products separated using a 20% polyacrylamide sequencing gel. PhosphorImager-generated histograms from the gel compare the fragmentation patterns for a set of degradation reactions using [^{1}H]- and [^{2}H]GA-1 . The histograms were normalized upon the area of the peak corresponding to cleavage at T_{28}.

observation of a common isotope effect on ss- and ds-cleavage events, not measurable by the nondenaturing method, suggests that these two events result from partitioning of a common intermediate subsequent to carbon–hydrogen bond cleavage.

The effect of deuterium substitution at the C-4′ position of a clearly definable 1° cleavage site was determined using GA-1 (Figure 3). The PhosphorImager-generated histograms for Fe-BLM degradation of [5′-^{32}P]- and [i-^{32}P]GA-1 are shown in Figure 5, panels a and b, respectively, and the computed values are shown in Table 4. Similar to the results obtained for GT-1 and GT-2, the isotope effect for ss-cleavage involving the 1° site, A_{33}, is equivalent to the effect observed upon formation of the corresponding ds-cleavage product ($A_{33} + T_{11}$ ds, 3.6 vs 3.9). While the isotope effects for A_{33} and A_{38} using [5′-^{32}P]- and [i-^{32}P]GA-1 should be identical, their differences can be rationalized based on two considerations. The first is that normalization with T_{28} is

Table 4: Sequence-Specific Isotope Effects on Fe-BLM Cleavage of GA-1 Deuteriated at the C-4′ of A_{33}

^{32}P-label	cleavage site	% product distribution [^{1}H][a]	% product distribution [^{2}H][b]	k_H/k_D (av)[c]
internal	A_{33} ss[d]	1.4	0.31	3.6 ± 0.4
internal	($A_{33} + T_{11}$) ds	0.31	0.07	3.9 ± 0.5
internal	T_{28}[e]	3.9	3.3	1.0
5′	A_{33}	1.2	0.24	5.8 ± 0.5
5′	T_{28}[f]	4.0	4.9	1.0
5′	T_{11}	0.53	0.36	1.9 ± 0.2

[a] The product distribution shown is for one set of reactions employing 25 μM Fe-BLM. The total degradation of [^{1}H]-[i-^{32}P]GA-1 was 5.9%. The total degradation of [^{1}H]-[5′-^{32}P]GA-1 was 6.2%. [b] The product distribution shown is for one set of reactions employing 25 μM Fe-BLM. The total degradation of [^{2}H]-[i-^{32}P]GA-1 was 3.8%. The total degradation of [^{2}H]-[5′-^{32}P]GA-1 was 6.0%. [c] The average of 3 experiments employing 25 μM Fe-BLM. [d] This fragment may also include a minor amount of the ss-cleavage product from degradation at T_{11}. [e] The extents of cleavage observed with [i-^{32}P]GA-1 were normalized on the extent observed at this site. [f] The extents of cleavage observed with [5′-^{32}P]GA-1 were normalized on the extent observed at this site.

more difficult with the [5′-^{32}P]GA-1 (Figure 5a) than with the [i-^{32}P]GA-1 (Figure 5b), due to the congestion of the histogram. Second, the very large isotope effects observed make quantitation of the [^{2}H]GA-1 more difficult.

While the results obtained using GT-1 and GT-2 have provided new insight into the ds-cleavage process, they do not allow investigation of the hypothesis that there is an obligate order to most ds-cleavage events. The model shown in Figure 1 states that a good ss-cleavage site provides the 1° cleavage site, which then ultimately results in the 2° cleavage event. To investigate the question of ordered cleavage, the effects of deuterium substitution at the 1° sites of GA-1 and GC-1 (Figure 3) upon cleavage at the corresponding 2° site were evaluated. The ordered model predicts that an isotope effect at the 1° cleavage site should be completely transferred to the 2° cleavage site even though there is no deuterium at that position. Substitution of [^{2}H]-A_{33} does result in a reduced extent of cleavage at the 2° site, T_{11}, as reflected by the isotope effect of 1.9 (Table 4). However, in contrast to expectations based upon an obligate ordered mechanism, this effect is only half that expected based upon the effect of 3.9 at the ($A_{33} + T_{11}$) ds cleavage site. In addition, examination of the extent of ss- and ds-cleavage using these two [^{2}H]- and [^{1}H]-labeled hairpins (Table 4) suggests that while ^{2}H-substitution at A_{33} dramatically reduces the extent of ds-cleavage, the relative amount of ss-cleavage at T_{11} is increased. The reduced isotope effects at T_{11} relative to A_{33} and the greater extents of ss-cleavage with [^{2}H]-labeled materials relative to [^{1}H] materials strongly suggest that ss-cleavage can occur at the 2° hit site.

Similar experiments have been carried out with GC-1. The isotope effects observed upon Fe-BLM degradation of GC-1 are presented in Table 5. The isotope effects upon ss-cleavage at C_{34} (1.8) and ds-cleavage involving C_{34} and G_{12} (1.7) are, once again, indistinguishable within the experimental error. As with GA-1, the isotope effect at the 2° site, G_{12} (1.2), is less than that observed at the 1° site, C_{34} (1.8). Therefore, in contrast to the conclusions of Steighner and Povirk (1992), the studies with GA-1 and GC-1 indicate that ss-cleavage, and possibly ds-cleavage, can be initiated by chemistry at the 2° hit site. The ramifications of these

Table 5: Sequence-Specific Isotope Effects on Fe-BLM Cleavage of GC-1 Deuteriated at C_{34} and C_{37}

^{32}P-label	cleavage site	% product distribution [^{1}H][a]	% product distribution [^{2}H][b]	k_H/k_D (av)[c]
internal	C_{37} ss	2.02	0.82	2.9 ± 0.2
internal	C_{10} ss	1.76	1.78	1.0 ± 0.04
internal	C_{34} ss[d]	2.24	1.23	1.8 ± 0.1
internal	C_{13} ss	0.25	0.26	1.1 ± 0.1
internal	T_{15} ss[e]	1.65	1.67	1.0
internal	(G_{12} + C_{34}) ds	0.34	0.24	1.7 ± 0.1
5′	C_{37}	2.58	0.83	2.7 ± 0.2
5′	C_{34}	2.69	1.30	1.9 ± 0.1
5′	T_{15}[f]	2.29	1.83	1.0
5′	C_{13}	0.39	0.32	0.92 ± 0.02
5′	G_{12}	0.52	0.30	1.2 ± 0.1
5′	C_{10}	2.22	1.79	0.93 ± 0.1

[a] The product distribution shown is for one set of reactions employing 80 μM Fe-BLM. The total degradation of [^{1}H]-[i-^{32}P]GC-1 was 8.7%. The total degradation of [^{1}H]-[5′-^{32}P]GC-1 was 11%. [b] The product distribution shown is for one set of reactions employing 80 μM Fe-BLM. The total degradation of [^{2}H]-[i-^{32}P] GC-1 was 6.4%. The total degradation of [^{2}H]-[5′-^{32}P]GC-1 was 6.4%. [c] The average of 3 experiments employing 80 μM Fe-BLM. The error represents the standard deviation. [d] This fragment may also include a small contribution from ss-cleavage occurring at G_{12}. [e] The extents of cleavage observed with [i-^{32}P]GC-1 were normalized on the extent observed at this site. [f] The extents of cleavage observed with [5′-^{32}P]GC-1 were normalized on the extent observed at this site.

studies will be discussed subsequently in the context of the model in Figure 1.

O_2 Dependence on Ds-Cleavage. The requirement for oxygen to produce ds-breaks by "activated BLM" generated *ex situ* was determined directly using hairpin oligonucleotides under anaerobic conditions. Subsequent to incubation with "activated BLM", the reaction mixtures were treated with 1 M piperidine or 10 mM putrescine (pH 8), to effect strand scission from the abasic sites (Figure 1), and analyzed by gel electrophoresis. The results of a typical experiment using [i-^{32}P]GT-1 are shown in Figure 6a, with a corresponding histogram of the gel shown in Figure 6b. The only observed fragments result from ss-cleavage. No ds-cleavage products are observed above background. These results establish that Fe-BLM-mediated ds-cleavage requires at least 1 equiv of oxygen over the amount required to form "activated BLM" and provide strong support for the mechanisms previously proposed by Povirk and co-workers (Povirk et al., 1989; Povirk and Houlgrave, 1988; Steighner & Povirk, 1990).

DISCUSSION

The model for BLM-mediated ds-cleavage shown in Figure 1 makes a number of predictions that have been tested experimentally. One prediction is that C-4′ hydrogen abstraction initiates chemistry at both the 1° and 2° cleavage sites. The results obtained using native gels to observe the ds-cleavage products indicate that an isotope effect accompanies ds-cleavage when either the 1° or 2° cleavage sites are deuteriated in the C-4′ position (Figure 2). These results strongly support the proposal that ds-cleavage involves C-4′ hydrogen abstraction from both sites involved in ds-cleavage. In conjunction with the characterization by denaturing gels of the DNA products of ds-cleavage (Povirk et al., 1989; Steighner & Povirk, 1990), it is reasonable to conclude that the detailed chemistry involved in the degradation of the individual nucleotides is equivalent to that proposed for ss-cleavage induced by Fe-BLM (Burger et al., 1986; McGall et al., 1992; Rabow et al, 1990; Murugeson et al., 1985; Sugiyama et al., 1985).

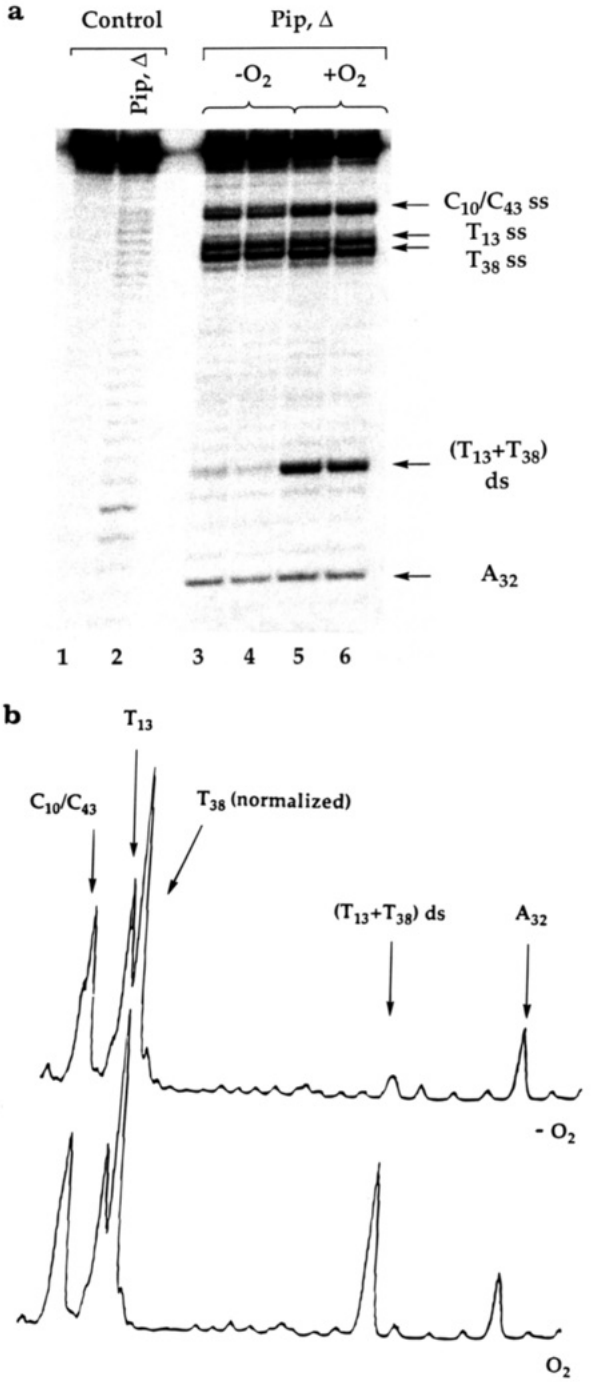

FIGURE 6: (a) Fe-BLM cleavage of [i-^{32}P]GT-1 under aerobic and anaerobic reaction conditions. "Activated BLM" was formed *ex situ* and added to [i-^{32}P]GT-1 under aerobic (+O_2) or anaerobic (−O_2) conditions and the products separated using a 20% polyacrylamide sequencing gel. The concentration of Fe-BLM in each reaction is as follows: lanes 1 and 2, no Fe-BLM; lanes 3−6, 12.5 μM Fe-BLM. The reaction mixtures in lanes 2−6 were treated with 1 M piperidine at 95 °C for 15 min prior to electrophoresis. (b) Histograms showing oxygen dependence upon the Fe-BLM-mediated ds-cleavage product in [i-^{32}P]GT-1. PhosphorImager-generated histograms for the reactions shown in lanes 4 (−O_2) and 5 (+O_2) in panel a were normalized upon the peak corresponding to ss-cleavage occurring at T_{38}.

On the basis of analysis of the ds cleavage products on denaturing gels, Povirk and co-workers concluded that ds-

cleavage requires O_2-dependent degradation at the 1° site (Povirk et al., 1989; Steighner & Povirk, 1990). To confirm this requirement, ds-cleavage was examined under anaerobic conditions. As indicated in Figure 6, essentially no ds-cleavage products were detected from reactions deprived of oxygen whether the workup was done directly or subsequent to alkaline treatment. If a single molecule of BLM is sufficient for the ds-cleavage process, these results are consistent with the mechanism in Figure 1 which requires an oxygenated intermediate involved in the degradation of the first strand to "reactivate" the Fe-BLM product for a second round of chemistry at a second site. The results are also consistent with an alternative mechanism for ds-cleavage described by Keller and Oppenheimer (1987) in which oxygen-dependent degradation produces an immediate strand break, thereby potentiating the binding of a second molecule of "activated BLM". Their original proposal assumed that the negatively charged products of ss-cleavage enhanced the binding of the second FeBLM, inconsistent with the kinetics of strand scission previously reported (Burger et al., 1986). A variation of their proposal, however, might employ a negatively charged intermediate in the production of the ss-break to enhance binding of a second FeBLM (Burger et al., 1986; McGall et al., 1992). While this model still cannot be fully discounted, results of Absalon et al. (1995), examining the ratio of ss- to ds-cleavage as a function of BLM concentration and the inability of Co-BLM to significantly perturb this ratio, in conjunction with earlier studies (Povirk, 1983; Povirk et al., 1977), allow us to favor a mechanism in which one molecule of Fe-BLM is responsible for both strand breaks.

A third mechanism for ds-cleavage which explains the requirement for additional oxygen proposes that "activated BLM" intrinsically possesses the oxidation equivalents required to effect two hydrogen atom abstractions. Studies by Burger et al. (1985) have demonstrated that "activated BLM" requires two reducing equivalents to form Fe(III)-BLM, the observed end product of FeBLM-mediated DNA degradation. Hydrogen abstraction by "activated BLM" or a Fe-BLM−oxene provides only one of these equivalents. In the absence of oxygen, a second reduction to yield Fe(III)-BLM can accompany the formation of the C-4′ hydroxylated nucleotide (Rabow et al., 1990). However, nucleotide degradation through the oxygen-dependent pathway leading to the 3′-phosphoglycolate-modified ends does not provide this second reducing equivalent, leaving open the possibility that the one-electron-reduced "activated BLM" may be able to effect a second hydrogen abstraction from a neighboring site. At present, this proposal has no precedent in the mechanistic literature on either proteins or model systems that effect hydroxylations of unactivated carbon−hydrogen bonds. Our present results do not allow a distinction to be made between this mechanism and the one shown in Figure 1, but if a single BLM molecule is indeed responsible for the production of a ds-break, the requirement for O_2 has important ramifications regarding the structure and the oxidation state of the BLM species directly involved in C-4′ hydrogen abstraction.

New Insight into the Ds-Cleavage Process. In addition to supporting the prevalence of C-4′ chemistry in the ds-cleavage process, the isotope effects observed using the [i-^{32}P]hairpins (Tables 2−5) provide us with new insight into the details of the mechanism of ds-cleavage by Fe-BLM. Previous observations of identical isotope effects on the oxygen-dependent and -independent ss-cleavage products generated when "activated BLM" interacted with DNA provided strong support for the proposal that they resulted from a partitioning of a common C-4′ radical intermediate (Kozarich et al., 1989; Worth et al., 1993; Wu et al., 1985). The simplest interpretation of the identical isotope effects upon the formation of ss- and ds-cleavage products with all four hairpins is that the two degradation pathways also partition from a common C-4′ radical intermediate. Since C-4′ hydrogen abstraction occurs subsequent to formation of an initial DNA-activated BLM complex, these results also suggest that both pathways employ the same initial binding mode. Thus, in contrast to the predictions of Steighner and Povirk (1990), different modes for BLM bound to DNA at the 1° site need not be invoked as a factor which directs the outcome of ss- vs ds-cleavage.

The conditions for the above interpretation, however, rely in part upon the assumption that cleavage at the 1° sites is a prerequisite for cleavage at the 2° site as shown in Figure 1. Therefore, we have also applied our isotope effect methodology to re-evaluate the sequential order of the cleavage events leading to a ds-break. If 1° site cleavage is imperative for 2° site cleavage to occur, then any reduction in cleavage at the 1° site by isotopic substitution should result in an identical extent of reduction in the cleavage observed at the 2° site. Examples of these "remote" isotope effects were sought using [5′-^{32}P]GA-1 and -GC-1, since the ds-cleavage characterized in these hairpins involve degradation at clearly discernible 1° and 2° sites. Comparison of the histograms shown in panels a and b of Figure 5 for the degradation of [5′-^{32}P]- and [i-^{32}P]GA-1, respectively, reveals that the reduction in cleavage observed at T_{11}, the 2° cleavage site, is less than ~1/2 the extent observed for A_{33} ss- or ds-cleavage (Table 4). A similar phenomenon is observed for Fe-BLM degradation of GC-1 (compare the effects reported for G_{12} with those observed for ss- and ds-cleavage involving C_{34}, Table 5). These results clearly indicate that cleavage at the 2° sites, T_{11} of GA-1 and G_{12} of GC-1, can occur without prior C-4′ hydrogen abstraction from the corresponding 1° sites (A_{33} of GA-1 and C_{34} of GC-1) and leave open the possibility that the cleavage events leading to a ds-break can occur in random-sequential order. Therefore, degradation at minor (2°) cleavage sites is not simply the result of a perturbed DNA structure due to a previous strand break as might be inferred in the mechanism proposed by Keller and Oppenheimer (1987).

While eliminating the requirement of prior 1° site cleavage for subsequent 2° site degradation, the isotope effects obtained using [5′-^{32}P]GA-1 and -GC-1 do not necessarily contradict the order stated in Figure 1 for ds-cleavage. The order of cleavage events may technically be described as random, yet at [^{1}H] sites a kinetic preference in which cleavage first occurs at the 1° site may also exist. In addition, chemistry that normally occurs at A_{33} of GA-1 may be diverted to the 2° site (T_{11}) when deuterium is substituted at C-4′ of A_{33}. This possibility, therefore, precludes unambiguous determination of the contribution to ds-cleavage by pathways which are initiated by cleavage at either the 1° or 2° site.

While the strict interpretation of the isotope effects is complex for the reasons outlined above, the observed trends allow us to favor and provide further support for a model

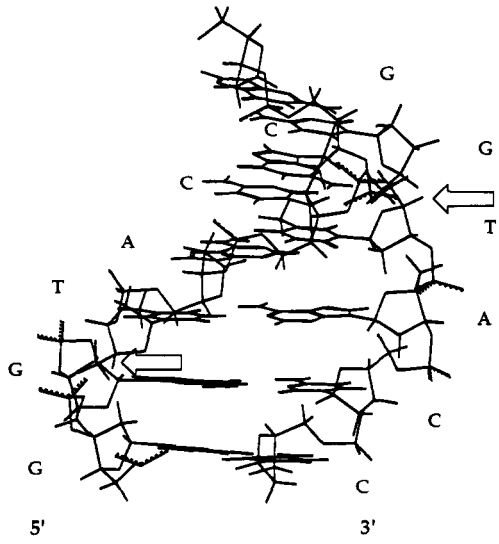

FIGURE 7: The two thymidine C-4′ hydrogens involved in ds-cleavage at 5′-GTAC/5′-GTAC. The minor groove of the sequence, 5′-(GGTACC)$_2$, was modeled in the B-form using *Insight II* molecular modeling system. The two C-4′ hydrogens involved in ds-cleavage are indicated with arrows. The calculated distance between the two hydrogens through the axis of the DNA is 18.4 Å.

similar to that originally proposed by Povirk and co-workers (Figure 1) (Povirk et al., 1989; Steighner & Povirk, 1990). We believe that the predominant ds-cleavage event is initiated at the 1° cleavage site by a mechanism identical to that observed for ss-cleavage by BLM. While our studies indicate that ds-cleavage can potentially be initiated at an unfavorable BLM ss-cleavage site, implying a random order mechanism, this order probably takes place much less frequently. We therefore suggest that the equivalence of the isotope effects on ss- and ds-cleavage indicates that both processes proceed through a common pathway involving C-4′ hydrogen atom abstraction of the targeted nucleotide and perhaps through the common peroxyl radical and/or hydroperoxide intermediate(s) in the oxygen-dependent degradation pathway (Burger et al., 1986; McGall et al., 1992).

Our investigations allow us to comment upon factors which may be responsible for the differences in the relative efficiencies of Fe-BLM-mediated ds-cleavage at the different sequences. The case study approach for measuring the efficiency of site-specific ds-cleavage described in the preceding paper revealed a ss/ds cleavage ratio of ~3.3 in GT-1 and GT-2, which differed significantly from other cleavage sites in the same hairpins and from cleavage sites in GA-1 and GC-1 (Absalon et al., 1995). Clearly, reactivation is one possible factor in a mechanism for ds-cleavage mediated by a single molecule of Fe-BLM. At present it is not possible to determine whether the efficiency of reactivation differs between individual ss-cleavage sites or if it is intrinsic to the mechanism for oxygen-dependent DNA degradation. An interesting implication, particularly in the latter case, is that Fe-BLM may again be reactivated after the second cleavage event (yielding phosphoglycolate at both 1° and 2° sites), making it chemically competent to initiate a third hydrogen abstraction from the DNA. Unfortunately, we have not been able, using this system, to detect multiple turnovers associated with a single activated BLM.

Clearly, another essential factor in ds-cleavage by a single molecule of BLM is the reorganization that must occur for a reactivated Fe-BLM to reach the second site of cleavage. The two C-4′ hydrogens involved in double-strand cleavage at a site such as 5′-GTAC/ 5′-GTAC are separated by ~18.4 Å and are located on opposite sides of a B-form DNA helix (Figure 7). Thus it may seem a challenge for a reactivated Fe-BLM molecule to traverse the required distance from the first cleavage site to the second site. Reactivated drug apparently does not diffuse far enough away from the DNA to join the free pool of Fe-BLM in its course to the second site of cleavage, since this action would be inconsistent with the experimentally observed Fe-BLM concentration independence upon the observed ss/ds-cleavage ratios (Absalon et al., 1995; Povirk et al., 1977). Efficient ds-cleavage may therefore occur in sequences which facilitate rearrangement of the BLM without requiring a complete dissociation of the molecule from the DNA. At present it seems unlikely that a BLM/DNA complex in which the BLM bithiazoles are extended in the minor groove of the DNA would lead to ds-cleavage. Assuming that the second C-4′ hydrogen abstraction leading to a ds-break requires a complete 180° reorientation of the BLM in the minor groove, an extended BLM structure would imply that all initial contacts be severed between BLM and the DNA prior to the reorganization. Such a situation would most probably lead to the observation of the ss/ds-cleavage ratio being dependent upon Fe-BLM concentration.

A more appealing model for a BLM/DNA complex which can effect both ss- and ds-cleavage might involve a compact BLM structure in which the bithiazoles, or positively charged tail of BLM, remain tightly associated with the DNA between the two cleavage sites. The metal binding moiety of BLM, still tethered to the DNA via its peptide linker, might then be allowed to reach the C-4′ hydrogen at both cleavage sites. Such an interaction is consistent with recent experiments asserting a role for the metal binding region of BLM in determining the sequence selectivity of ss-cleavage (Carter et al., 1990, 1991; Kane et al., 1994). Furthermore, a recent preliminary structure of CoBLM-A$_2$ (green) in the presence of the self-complementary oligonucleotide d(CCAGGC-CTGG)$_2$, containing a single CoBLM cleavage site, has been determined by 2D NMR methods. These studies suggest that the bithiazoles bind by intercalation from the minor groove on the 3′ side of the dC undergoing cleavage (Wu et al., 1994). The linker from the metal binding domain to the bithiazoles could thus provide the flexibility essential for the reorganization required to mediate cleavage at the 2° site. The bithiazoles would remain intercalated during this process. This model also explains why ds-cleavage at the dCs in (5′-GC/5′-GC) is not observed. Interesting results of Boger et al. (1994) support the importance of the peptide linker in BLM's tail to the efficiency of ds-cleavage. Further insight into the rearrangement of Fe-BLM in the DNA minor groove will benefit from the detailed solution of this CoBLM/DNA complex structure by NMR methods. Work in this area is in progress.

REFERENCES

Absalon, M. J., Krishnamoorthy, C. R., McGall, G., Kozarich, J. W., & Stubbe, J. (1992) *Nucleic Acids Res. 20*, 4179−4185.

Absalon, M. J., Kozarich, J. W., & Stubbe, J. (1995) *Biochemistry 34*, 2065−2075.

Ajmera, S., Massof, S., & Kozarich, J. W. (1986) *J. Labelled Compd. Radiopharm. 23*, 963−968.

Boger, D. L., Honda, T., Menezes, R. F., Colletti, S. L., Dang, Q., & Yang, W. (1994) *J. Am. Chem. Soc. 116*, 82−92.
Burger, R. M., Peisach, J., & Horwitz, S. B. (1981) *J. Biol. Chem. 256*, 11636−11644.
Burger, R. M., Blanchard, J. S., Horwitz, S. B., & Peisach, J. (1985) *J. Biol. Chem. 260*, 15406−15409.
Burger, R. M., Projan, S. J., Horwitz, S. B., & Peisach, J. (1986) *J. Biol. Chem. 261*, 15955−15959.
Carter, B. J., Murty, V. S., Reddy, K. S., Wang, S.-N., & Hecht, S. M. (1990) *J. Biol. Chem. 265*, 4193−4196.
Carter, B. J., Reddy, K. S., & Hecht, S. M. (1991) *Tetrahedron 47*, 2463−2474.
D'Andrea, A. D., & Hasetine, W. A. (1978) *Proc. Natl. Acad. Sci. U.S.A. 75*, 3608−3612.
Dedon, P. C., & Goldberg, I. H. (1992) *Chem. Res. Toxicol. 5*, 311−332.
Dervan, P. B. (1986) *Science 232*, 464−471.
Fox, K. R. (1990) *Anti-Cancer Drug Des. 5*, 99−104.
Kane, S. A., Natrajan, A., & Hecht, S. M. (1994) *J. Biol. Chem. 269*, 10899−10904.
Keller, T. J., & Oppenheimer, N. J. (1987) *J. Biol. Chem. 262*, 15144−15150.
Kozarich, J. W., Worth, L., Jr., Frank, B. L., Christner, D. F., Vanderwall, D. E., & Stubbe, J. (1989) *Science 245*, 1396−1399.
Krishnamoorthy, C. R., Vanderwall, D. E., Kozarich, J., & Stubbe, J. (1988) *J. Am. Chem. Soc. 110*, 2008−2009.
Kuwahara, J., & Sugiura, Y. (1988) *Proc. Natl. Acad. Sci. U.S.A. 85*, 2459−2463.
McGall, G. H., Rabow, L. E., Ashley, G. W., Wu, S. H., Kozarich, J. W., & Stubbe, J. (1992) *J. Am. Chem. Soc. 114*, 4958−4967.
Murugeson, N., Xu, C., Ehrenfeld, G. M., Sugiyama, H., Kilkuskie,R. E., Rodriguez, L. O., Chang, L. H., & Hecht, S. M. (1985) *Biochemistry 24*, 5735.
Povirk, L. F. (1983) *Bleomycin*, in *Molecular Aspects of Anti-Cancer Drug Action* (Neidle, S., & Waring, M., Eds.) Vol. 3, pp 157−181, Macmillan, London.
Povirk, L. F., & Houlgrave, C. W. (1988) *Biochemistry 27*, 3850−3857.
Povirk, L. F., Wübker, W., Köhnlein, W., & Hutchinson, F. (1977) *Nucleic Acids Res. 4*, 3573−3580.
Povirk, L. F., Han, Y.-H., & Steighner, R. J. (1989) *Biochemistry 28*, 5808−5814.
Rabow, L. E., Stubbe, J., & Kozarich, J. W. (1990) *J. Am. Chem. Soc. 112*, 3196−3203.
Sam, J. W., Tang, X.-J., & Peisach, J. (1994) *J. Am. Chem. Soc. 116*, 5250−5256.
Sambrook, J., Fritsch, E. F., & Mantiatis, T. (1989) *Molecular Cloning: A Laboratory Manual*, Cold Spring Harbor, Laboratory Press, Cold Spring Harbor, NY.
Steighner, R. J., & Povirk, L. F. (1990) *Proc. Natl. Acad. Sci. U.S.A. 87*, 8350−8354.
Stubbe, J., & Kozarich, J. W. (1987) *Chem. Rev. 87*, 1107−1136.
Sugiura, Y., & Suzuki, T. (1982) *J. Biol. Chem. 257*, 10544−10546.
Sugiyama, H., Xu, C., Murugesan, N., & Hecht, S. M. (1985) *J. Am. Chem. Soc. 107*, 4104.
Worth, L., Jr., Frank, B. L., Christner, D. F., Absalon, M. J., Stubbe, J., & Kozarich, J. W. (1993) *Biochemistry 32*, 2601−2609.
Wu, J. C., Kozarich, J. W., & Stubbe, J. (1985) *Biochemistry 24*, 7562−7568.
Wu, W., Vanderwall, D. E., Stubbe, J. Kozarich, J. W., & Turner, C. J. (1994) *J. Am. Chem. Soc. 116*, 10843−10844.
Xu, R. X., Nettesheim, D., Otvos, J. D., & Petering, D. H. (1994) *Biochemistry 33*, 907−916.

BI941840R